

Simple one-step synthesis of highly luminescent carbon dots from orange juice: Application as excellent bio-imaging agents

Swagatika Sahu,^a Birendra Behera,^b Tapas K. Maiti,^b and Sasmita Mohapatra^{*a}

Electronic Supplementary Information

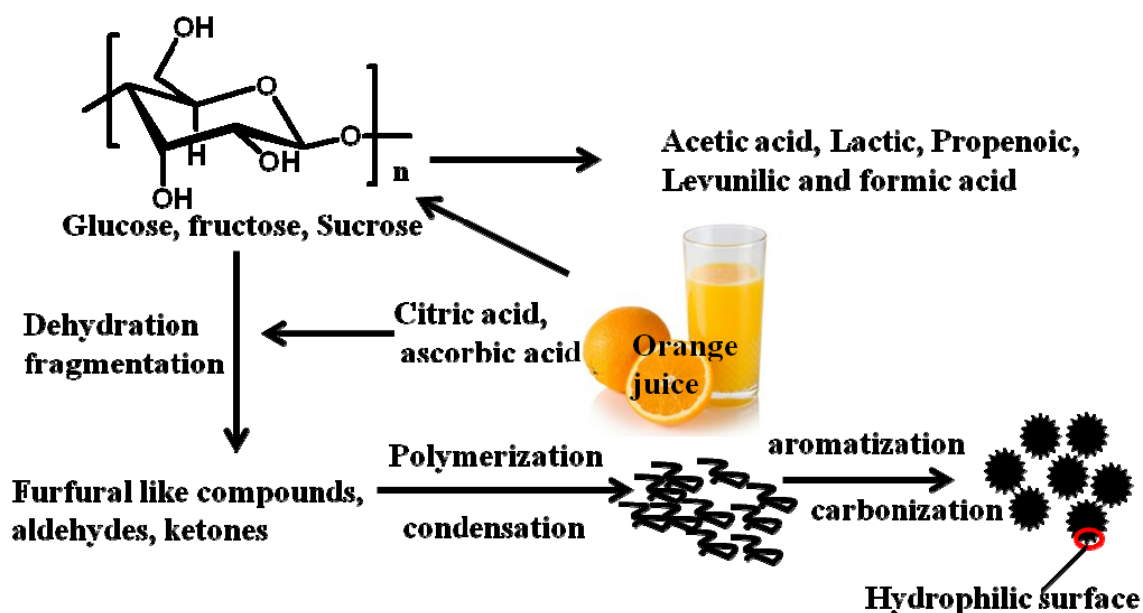
Experimental

Synthesis of carbon nanoparticles

Carbon nanoparticles were synthesized by hydrothermal treatment of orange juice in ethanol. In a typical procedure, 40 ml of orange juice (absolutely pulp-free) was mixed with 30 ml ethanol, and then the mixture was transferred into an 80 ml Teflon-lined stainless-steel autoclave and was heated at constant temperature of 120 °C for 150 min (1 °C/min). After the reaction is over, the autoclave was cooled down naturally. The resulted dark brown solution was washed with dichloromethane to remove the unreacted organic moieties. The aqueous solution was centrifuged at 3000 rpm for 15 min to separate the less-fluorescent deposit. Excess acetone was added to the upper brown solution and centrifuged at high speed of 10,000 rpm for 15 min to obtain highly fluorescent carbon dots (CD, 400 mg) of average size 1.5-4.5 nm. The deposit coarse nanoparticles (CP, 250 mg) have larger diameters in the range of 30-50 nm and exhibit weak fluorescence in comparison to CD.

Plausible mechanism for the formation of carbon dots

The mechanism for synthesis of carbon dots from orange juice involves carbonization of its constituents. In fact, in the hydrothermal carbonization of sucrose for the formation of final material structure is complicated and a clear scheme has not yet been reported. The plausible mechanism for the formation of carbon dots may be illustrated as follows.



Schematic presentation of formation mechanism of carbon dots

Sucrose when hydrothermally treated undergoes hydrolysis to form glucose and fructose. Glucose subsequently isomerises to form fructose. The dehydration and decomposition of fructose/glucose gives rise to different soluble products such as furfural compounds (for ex: 5-hydroxymethyl furfural, furfural, 5-methyl furfural etc), several organic acids such as acetic, lactic, propionic, livulinic and formic acids, aldehydes and phenols. It is worth mentioning that the hydronium ion formed from these acids acts as a catalyst in subsequent decomposition reaction stages. Here it is important to note that due to presence of weak acids like citric acid and ascorbic acid in orange juice the dehydration and decomposition reaction proceeds in a controlled manner. The polymerisation and condensation of of these products gives rise to soluble polymers. Aromatization and formation of aromatic clustures take place via aldol condensation, cycloaddition and a hydroxymethyl mediated furan resin condensation. When concentration of aromatic clusters reaches a critical supersaturation point a burst nucleation takes place and carbon dots are formed.

Ref:

1. M. Sevilla, A.B. Fuertes, *Carbon*, **2009**, *47*, 2281-2289.

2. B. Hu, K. Wang, L. Wu, S-H Yu, M. Antonietti, and M-M Titirici, *Adv. Mater.* **2010**, *22*, 813–828.

In vitro cytotoxicity and intracellular uptake

In vitro cytotoxicity

L929 cells were harvested and the cell concentration was adjusted to 1×10^4 cells/ml, cells were plated in a 96 well flat bottom culture plates (180 μ l/well) and incubated with various concentrations (0.78, 3.185, 12.5, 25.0, 50.0, 100.0, and 200.0 μ l/ml) of CD (in 20 μ l). All cultures were incubated for 72 h at 37 °C and 5% CO₂ in a humidified incubator. Viable cell concentration was checked by MTT (3-(4,5-Dimethyl-2-thiazolyl)-2,5-diphenyl-2H-tetrazolium bromide) assay.

Intracellular uptake

Human osteosarcoma cell line MG63 (maintained in Dulbecco's Modified Eagle's Medium or DMEM supplemented with 10% Fetal Bovine Serum or FBS) was trypsinized and seeded in tissue culture plates at 3×10^4 cells/well. After overnight incubation inside humidified 5% CO₂ incubator for cell attachment, the cells were treated with the CD at a final concentration of 200 μ g/ml in 300 μ l of media and incubated for 12 h. Prior to the imaging experiment, the cells were washed three times with fresh media. Live-cell-imaging was done under confocal microscope with laser excitation of 405 and 488 nm and fluorescence was collected in blue and green region.

Characterization

The morphology and microstructures of CD and CP were analyzed by Scanning electron microscope (HITACHI COM-S-4200) and High resolution transmission electron microscopy (JEOL 3010, Japan) operated at 300 kV respectively. Particle size and zeta potential were measured after suitable dilution of the CD solution at $25.0 \pm 0.5^\circ\text{C}$, by dynamic laser light scattering using a particle size analyzer (Nano ZS 90, Malvern). The crystalline phase was investigated by an Expert Pro Phillips X-ray diffractometer. The Raman spectrum of as-prepared samples was recorded at ambient temperature in a Ranishaw inVia relex spectrometer (UK

make). Fluorescence microscopy images were captured using Axiovert 40 Carl Zeiss India fluorescence microscope at excitation wavelength of 405 and 488 nm. The Fourier transform infrared spectroscopy (FTIR) spectra were measured by a Thermo Nicolet Nexux FTIR model 870 spectrometer with the KBr pellet technique ranging from 400 to 4000 cm^{-1} . The presence of different functional groups on the surface of CD was investigated by X-ray photoelectron spectroscopy using $\text{AlK}\alpha$ excitation source in an ESCA-2000 Multilab apparatus (VG microtech). Fluorescence spectroscopy was performed with a Horiba Fluoromax 4 spectrophotometer at different excitation wavelength ranging from 320 to 450 nm. UV-vis absorption spectra were obtained using a Shimadzu 220V (E) UV-vis spectrophotometer. Live-cell imaging was done under Olympus FV-1000 confocal microscope with laser excitations of 405 and 488 nm.

Figure S1

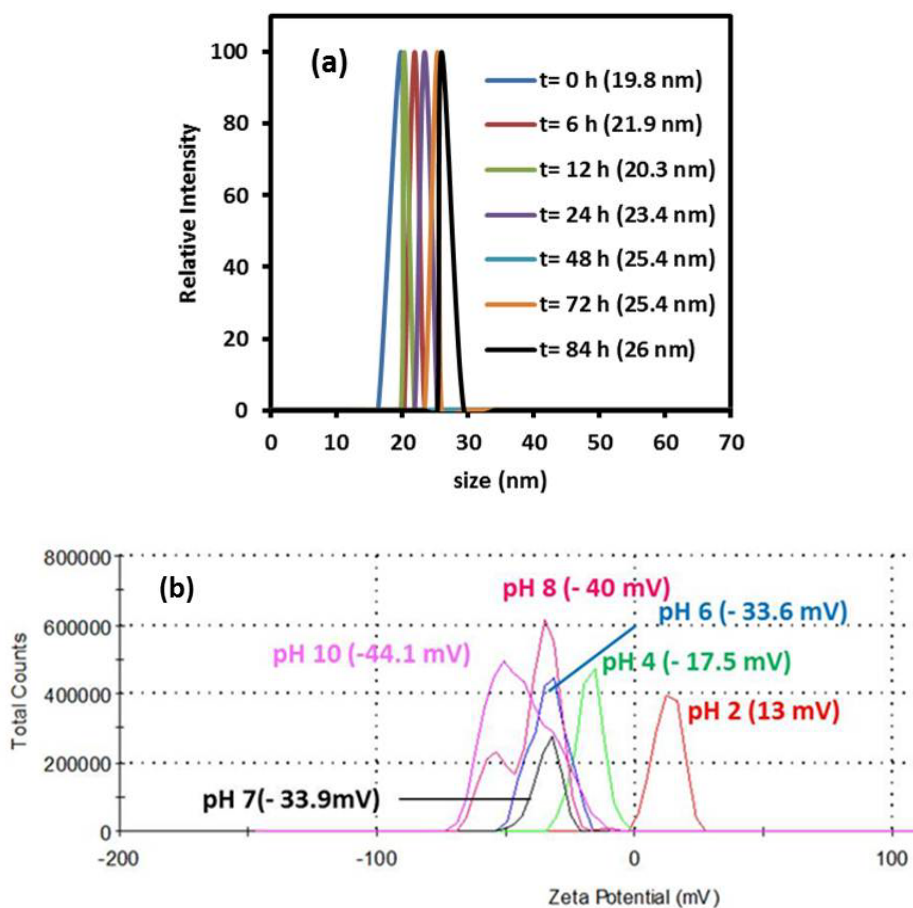


Figure S1. Variations of (a) hydrodynamic size with time, (b) zeta potential with pH.

Figure S2

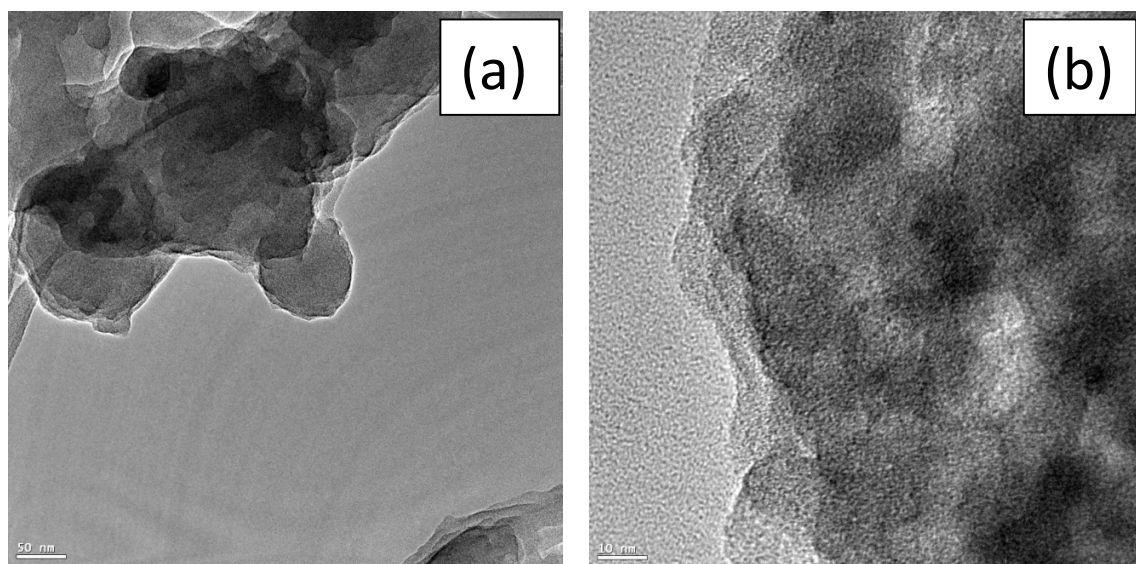


Figure S2 (a) and (b) TEM images of coarse particles

Figure S3

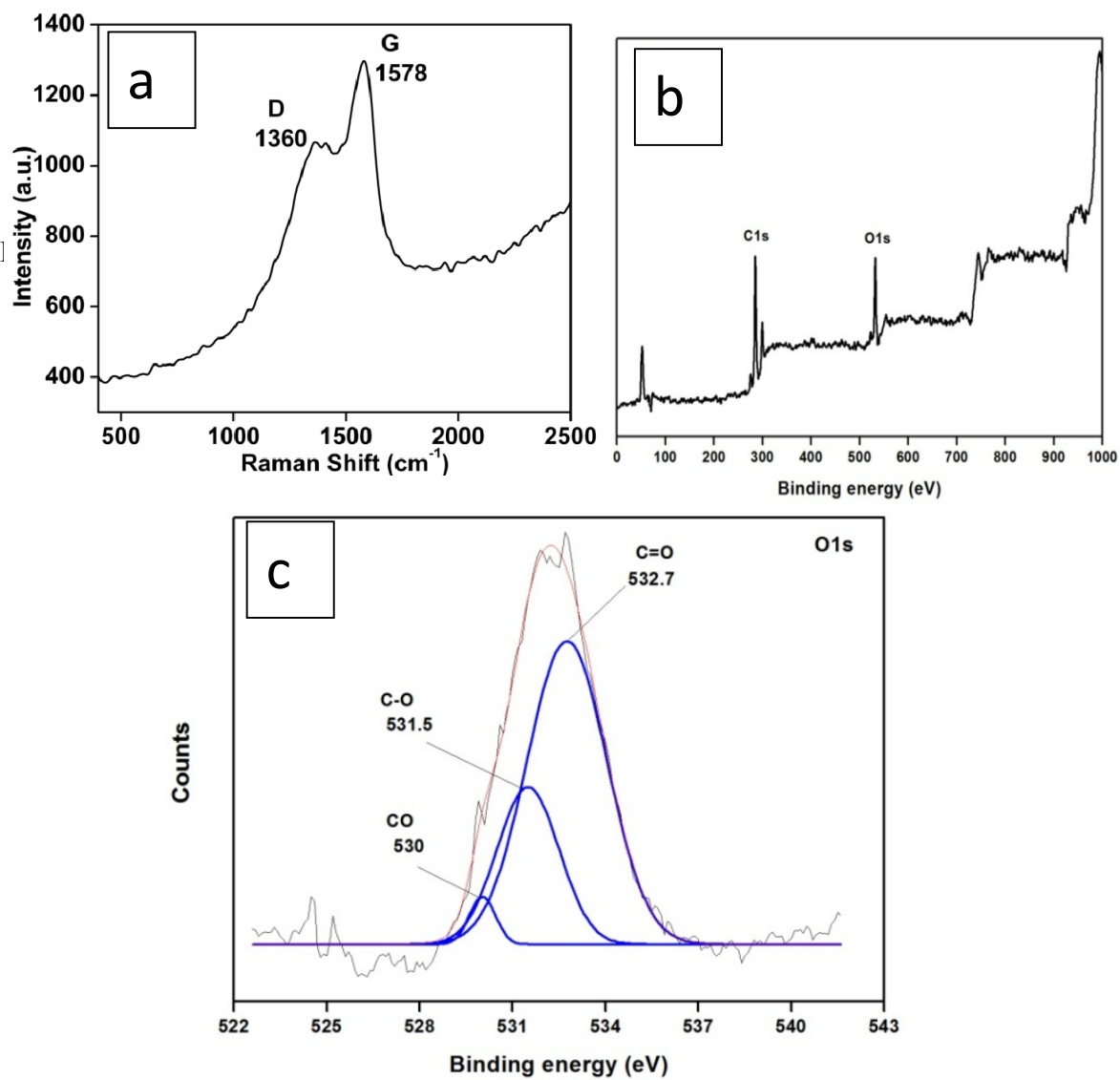


Figure S3 (a) Raman spectrum of CP, (b) XPS survey and (c) O1s spectrum of CD

Figure S4

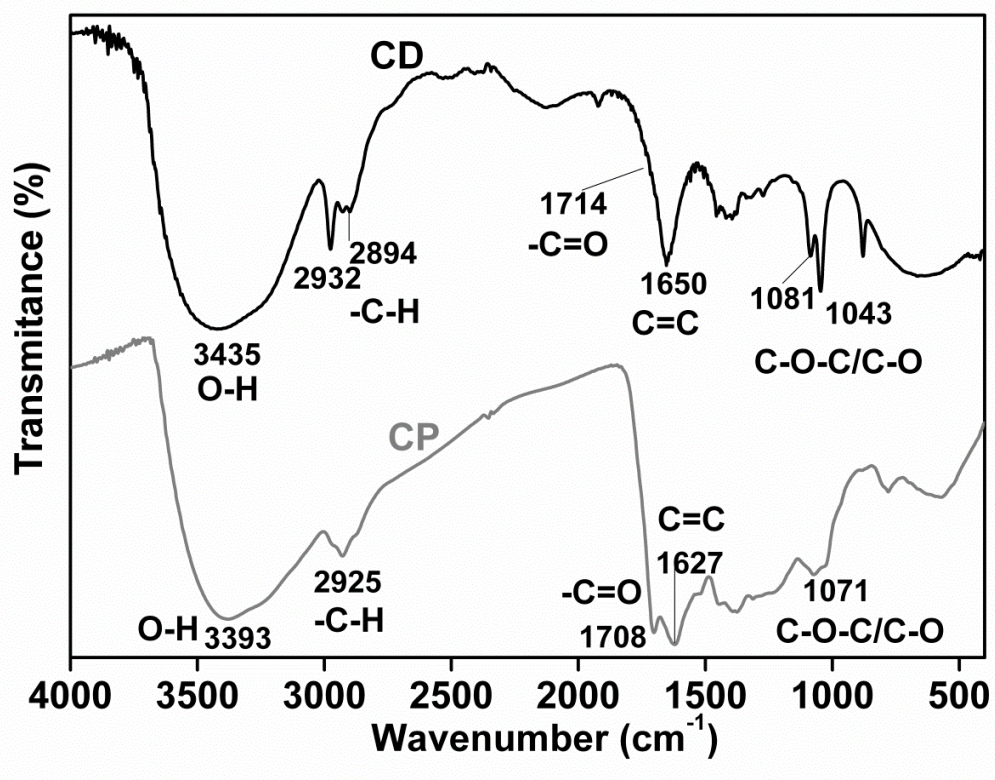


Figure S4 FTIR spectra of CD and CP

Figure S5.

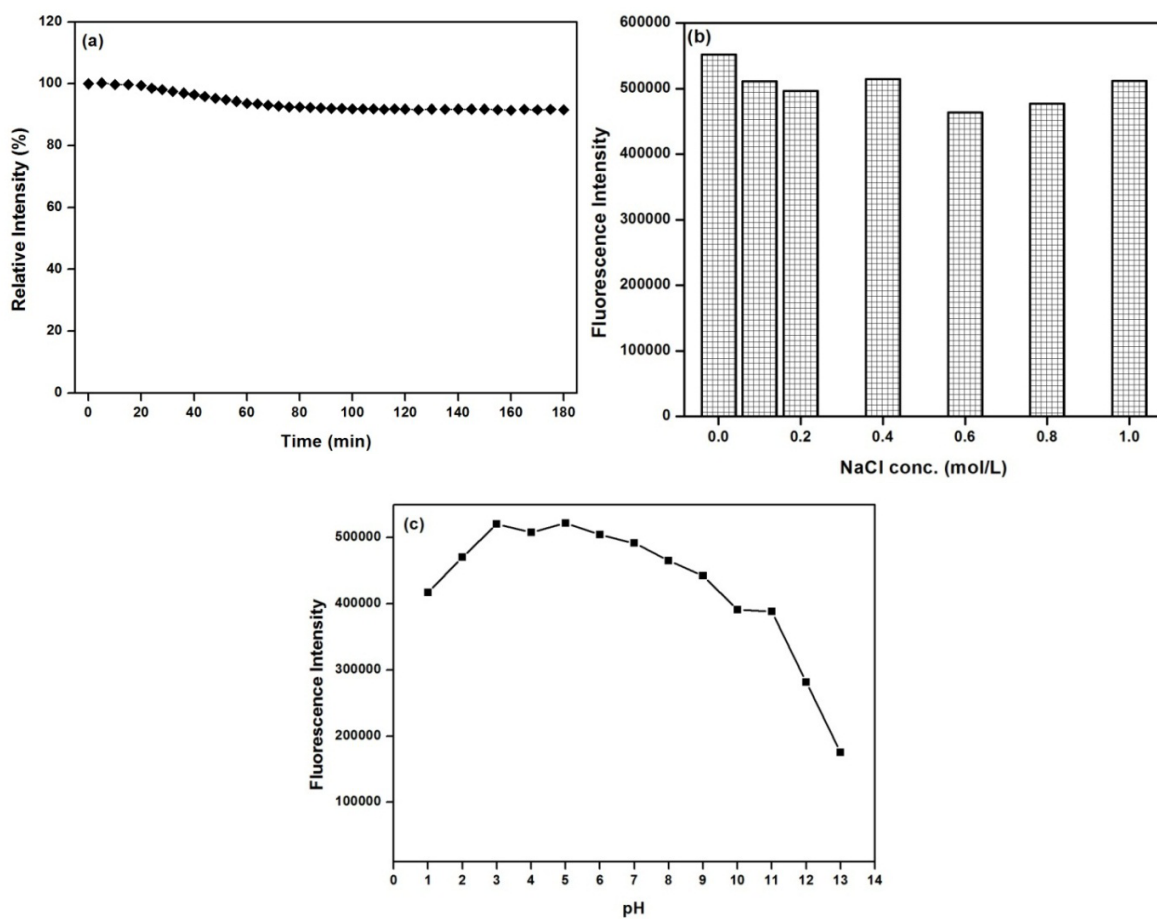


Figure S5 (a) Effect of time on fluorescence intensity of CD in DI water, (b) Effect of ionic strengths on the fluorescence intensity of CD (ionic strengths were controlled by various concentrations of NaCl), (c) Effect of pH on the fluorescence intensity of CD

Quantum Yield Calculations

The quantum yield (Φ) of the carbon nanoparticle was calculated using quinine sulfate as reference. For calculation of quantum yield, five concentrations of each compound were made, all of which had absorbance less than 0.1 nm at 340 nm. Quinine sulfate (literature $\Phi = 0.54$) was dissolved in 0.1 M H_2SO_4 (refractive index (η) of 1.33) while the carbon sample was dissolved in water ($\eta = 1.33$). Their fluorescence spectra were recorded at same excitation of 340 nm. Then by comparing the integrated photoluminescence intensities (excited at 340 nm) and the absorbency values (at 340 nm) of the carbon sample with the references quinine sulfate quantum yield of the carbon sample was determined. The data was plotted (Figure S4) and the slopes of the sample and the standards were determined. The data showed good linearity with intercepts of approximately zero.

The quantum yield was calculated using the below equation

$$\Phi_x = \Phi_{ST} (m_x / m_{ST}) (\eta_x^2 / \eta_{ST}^2)$$

Where Φ is the quantum yield, m is slope, η is the refractive index of the solvent, ST is the standard and X is the sample. The quantum yield for CD and CP is found to be 25.6 % and 19.7% respectively

Figure S6.

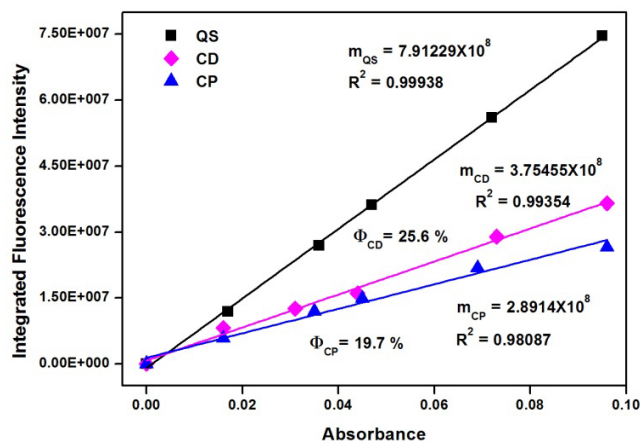


Figure S6 Fluorescence and Absorbance of the CD, CP and Quinine Sulfate

Ref:

1. D. Pan, J. Zhang, Z. Li, C. Wu, X. Yan, M. Wu, Chem. Commun., 2010, **46**, 3681.

2. J. Zhou, C. Booker, R. Li, X. Zhou, T. K. Sham, X. Sun, Z. Ding, J. Am. Chem. Soc., 2007, **129**, 744.

Figure S7

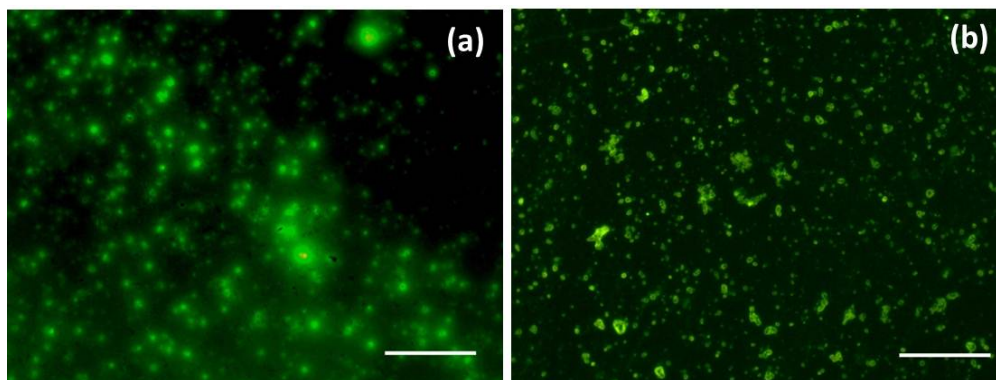


Figure S7. Typical Fluorescence microscopy images (all scale bars are 30 μm) of CD (a) and CP (b) with excitation wavelength at 488 nm

Figure S8

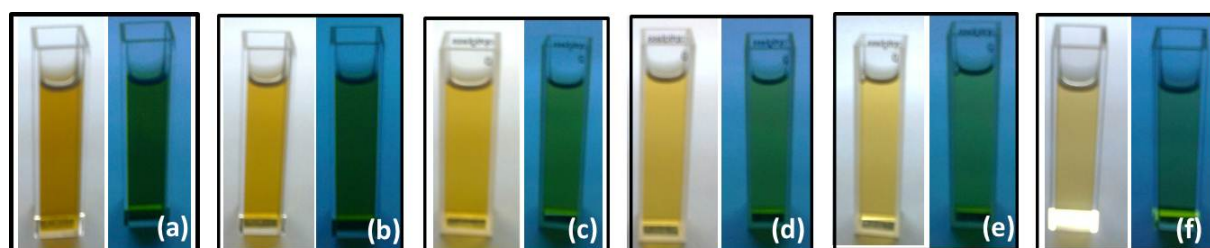


Figure S8. Photographs of CD in water under daylight (left) and UV lamp (right) with different concentrations of CD (a: 0.5 mg/ml, b: 0.34 mg/ml, c: 0.25 mg/ml, d: 0.17 mg/ml, e: 0.12 mg/ml, f: 0.08 mg/ml respectively)

Figure S9

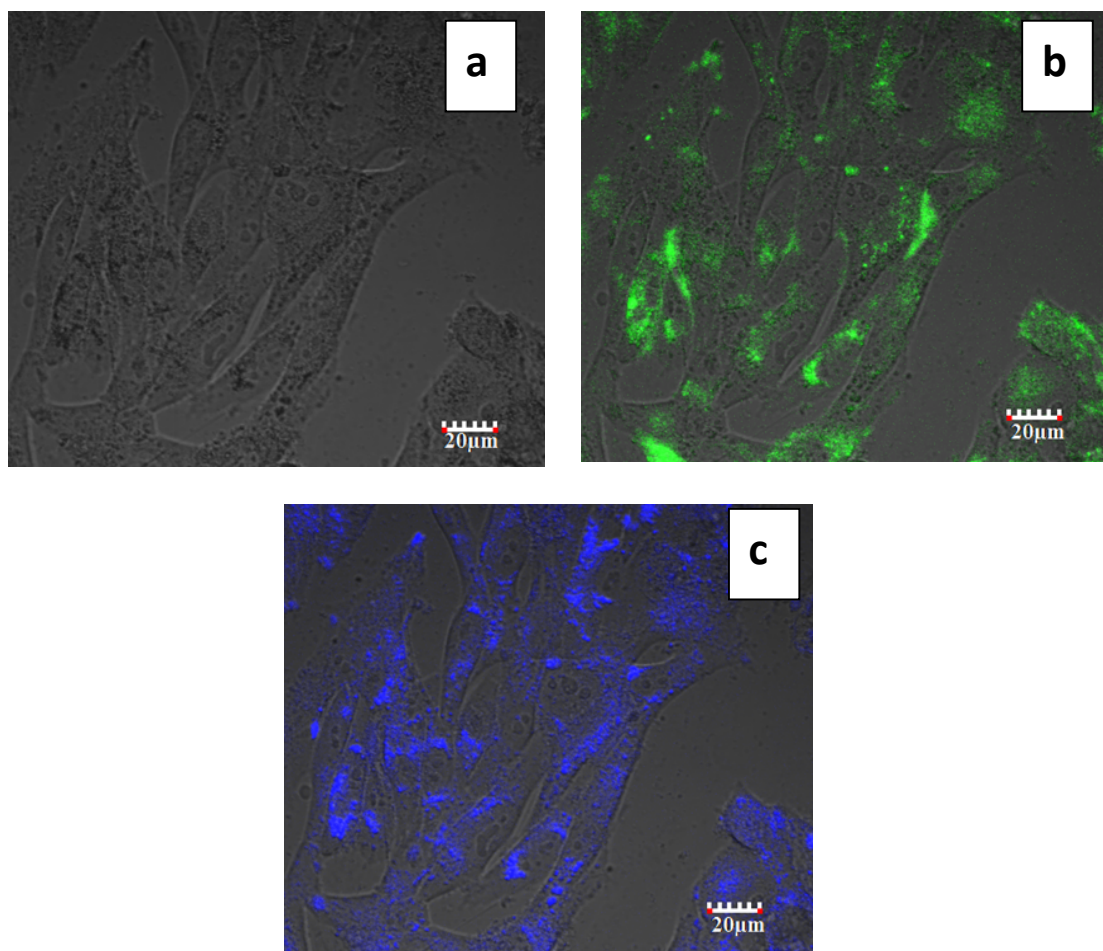


Figure S9 More cellular uptake images in MG-63 cells. (a) bright field, (b) at excitation 488 nm (c) at excitation 405 nm.